

# INFLUENCE OF PREPARATION CONDITIONS ON THE MORPHOLOGY OF Fe<sub>78</sub>Si<sub>9</sub>B<sub>13</sub> RIBBONS

*Milan Pavúk<sup>1</sup>, Narges Amini<sup>2</sup>, Marcel Miglierini<sup>1</sup>*

<sup>1</sup>*Institute of Nuclear and Physical Engineering, Slovak University of Technology  
in Bratislava, Ilkovičova 3, 812 19 Bratislava, Slovak Republic*

<sup>2</sup>*Department of Physics, Bu-Ali Sina University, 65174-4161 Hamedan, Iran*

*E-mail: milan.pavuk@stuba.sk*

*Received 16 April 2017; accepted 05 May 2017*

## 1. Introduction

The Fe<sub>78</sub>Si<sub>9</sub>B<sub>13</sub> metallic glass exhibit high saturation magnetization ( $> 130 \text{ A}\cdot\text{m}^2\cdot\text{kg}^{-1}$ ), high Curie temperature ( $> 400 \text{ K}$ ), and low coercivity which are desirable characteristics for soft ferromagnetic alloys. These properties are beneficial namely from an application point of view [1] suggesting these alloys as suitable candidates for transformer cores [2], magnetic shielding, sensors, etc.

Continuing interest in a classical Fe<sub>78</sub>Si<sub>9</sub>B<sub>13</sub> metallic glass can be documented for example by a recent work [3] in which this system was prepared under different quenching conditions and investigated from the perspective of its microstructure, magnetism, and electrochemical properties employing various techniques. Even though, the effect of quenching rate on the properties of amorphous alloys is continuously investigated [4,5], more information is needed to utilize these materials from magnetic application point of view.

This paper aims at determining the influence of quenching wheel speed on the surface morphology of Fe<sub>78</sub>Si<sub>9</sub>B<sub>13</sub> ribbons. The surfaces were studied by the Atomic Force Microscopy (AFM).

In general, the use of the Atomic Force Microscope in study of FeSiB alloys is quite rare [2,6-7]. Therefore, surface analysis using this sophisticated approach can be valuable for scientific community.

## 2. Experimental details

Metallic glasses with a nominal composition of Fe<sub>78</sub>Si<sub>9</sub>B<sub>13</sub> were produced by the method of rapid solidification of melt on a rotating wheel (chill block melt spinning). The castings were performed with tangential wheel speeds of 15 and 40 m/s, while keeping the other production parameters constant. The resulting ribbons were ~1.1 mm wide. Significant differences are observed in the ribbons thicknesses. While the alloy produced at 40 m/s has the thickness of only  $22.7 \pm 0.9 \text{ }\mu\text{m}$ , the alloy produced at 15 m/s is almost three times as thick ( $60.8 \pm 0.8 \text{ }\mu\text{m}$ ).

Prior to the AFM measurement, the ribbons were cleaned of organic impurities by immersing them in pure solvents. At first, they were immersed in tetrachloroethylene (99.9%) and later in isopropyl alcohol (99.8%). After cleaning they were left to dry in a desiccator.

The Dimension Edge™ (Veeco, USA) Atomic Force Microscope was used to obtain surface morphology of the ribbons. The microscope is placed on a pneumatic anti-vibration table and shielded with an acoustic cover during the measurements. Scanning was conducted in tapping mode. Due to highly reflective surface of the samples, a probe with reflective Al coating on the cantilever back side was used. This choice was made in order to reduce the optical interference. The surface of each ribbon was scanned at multiple locations to make sure that features observed in the image are characteristic for the given surface.

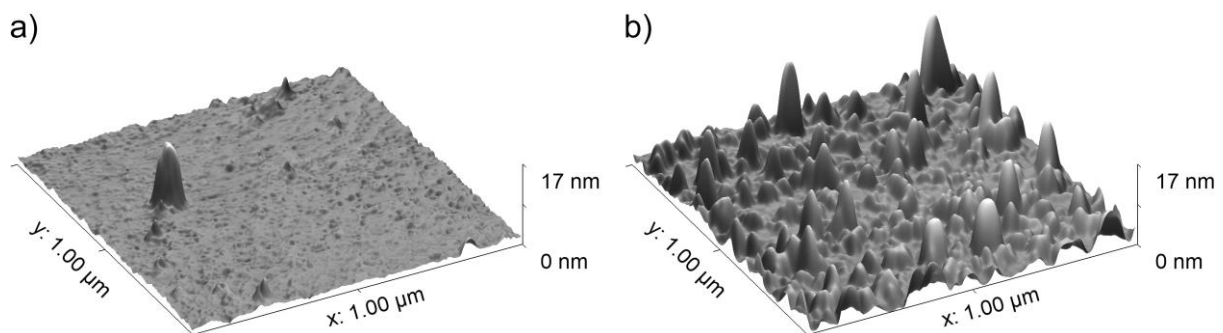
### 3. Results and discussion

Figure 1 depicts in 3-D the topography of both rapidly quenched  $\text{Fe}_{78}\text{Si}_9\text{B}_3$  alloys obtained by the AFM. The scanned area is  $1 \times 1 \mu\text{m}^2$ . The AFM scans were performed from the air exposed ribbon side, not that one in contact with the cooling wheel during the production process. On this side, the crystallization is assumed to start earlier, though there are exceptions from this rule [8].

As can be seen in Fig. 1a, the surface of the alloy produced at 40 m/s is smooth without substantial number of protrusions that would indicate the presence of crystalline phases. In fact, only one protrusion is present in the scanned area with the height of 13.3 nm. The average surface roughness excluding the tall protrusion is only 0.2 nm.

On the other hand, the alloy produced at 15 m/s (Fig. 1b) has the surface completely covered with protrusions. Most of them are small with the average height of 2.8 nm. However, there are also markedly larger protrusions with the average height of 11.8 nm. This indicates that the tangential wheel speed of 15 m/s is insufficient to support the formation of amorphous structure in the surface regions. Please remember that the ribbon produced at lower wheel speed is thicker what contributes to slower heat transfer.

A certain amount of crystalline bcc-Fe and  $\text{Fe}_3\text{Si}$  phases was detected by X-ray diffraction at the air exposed side of the ribbon produced at 15 m/s [9]. The results obtained from Mössbauer spectrometry of this ribbon are also interesting [9]. A component that would correspond to a crystalline phase was not observed in the corresponding Mössbauer spectra that were recorded both in the transmission and the emission mode providing information from the bulk and surface of the ribbon, respectively. What, however, could be observed in Mössbauer spectra quantitatively was the reorientation of the magnetic moments from random orientation in the bulk into strictly directional arrangement at the surface. Surface layers have magnetic moments aligned almost in the ribbon plane. According to the model proposed by Ok and Morrish [10], formation of crystalline surface layers with higher-density generates tensile stresses within the layers. This leads to the in-plane anisotropy observed in the conversion-electron Mössbauer spectrum. Therefore, the change in the orientation of magnetic moments in the ribbon produced at 15 m/s can indirectly point to the presence of some higher-density crystalline phases located at the very surface while the bulk of the ribbon remains amorphous. The above facts suggest that the protrusions seen in Fig. 1b are, in fact, nanocrystalline grains probably of bcc-Fe(Si) origin. It should be noted that surface crystallization is a known phenomenon in  $\text{Fe}_{78}\text{Si}_9\text{B}_{13}$  [10,11] and other metallic glasses [12] as well as some nanocrystalline alloys [8,13,14].



*Fig. 1: The AFM 3-D images of the as-produced  $\text{Fe}_{78}\text{Si}_9\text{B}_{13}$  metallic glass ribbons. The tangential wheel speed was: a) 40 and b) 15 m/s. These sides of the ribbons were not in contact with the quenching wheel. Both images are equally scaled in the z-direction. It should be noted that lateral dimensions of surface objects are affected by tip-sample convolution and therefore seem to be wider than they really are.*

#### 4. Conclusions

A comparison has been made between the two Fe<sub>78</sub>Si<sub>9</sub>B<sub>13</sub> ribbons produced at different tangential speeds of the quenching wheel. The ribbon produced at 40 m/s has the characteristics of an amorphous alloy. The surface of the alloy is smooth without tightly-packed protrusions that would indicate the presence of a crystalline fraction. On the other hand, the AFM measurements obtained from the as-quenched ribbon produced at 15 m/s provide solid indications that the alloy is not entirely amorphous. This leads to the conclusion that the operation of melt spinning at tangential wheel speed of 15 m/s is not suitable for production of Fe<sub>78</sub>Si<sub>9</sub>B<sub>13</sub> metallic glass when surface amorphicity is required.

#### Acknowledgement

This work was financially supported by grant of the Science and Technology Assistance Agency no. APVV-16-0079 and the Scientific Grant Agency of the Ministry of Education of Slovak Republic and the Slovak Academy of Sciences no. VEGA-1/0339/16.

#### References:

- [1] O. Gutfleisch, M. A. Willard, E. Brück, C. H. Chen, S. G. Sankar, J. P. Liu: *Adv. Mater.* **23**, 821 (2011).
- [2] Z. Li, Y. Dong, F. Li, C. Chang, X. M. Wang, R. W. Li: *J. Mater. Sci.: Mater. Electron.* **28**, 1180 (2017).
- [3] L. L. Meng, X. Y. Li, J. Pang, L. Wang, B. An, L. J. Yin, K. K. Song, W. M. Wang: *Metall. Mater. Trans. A* **44**, 5122 (2013).
- [4] Y. G. Su, F. Chen, C. Y. Wu, M. H. Chang, C. A. Chung: *ISIJ Int.* **55**, 2383 (2015).
- [5] S. Sohrabi, H. Arabi, A. Beitollahi, R. Gholamipour: *J. Mater. Eng. Perform.* **22**, 2185 (2013).
- [6] M. Coisson, F. Celegato, E. Olivetti, P. Tiberto, F. Vinai, M. Baricco: *J. Appl. Phys.* **104**, 033902 (2008).
- [7] Z. G. Sun, H. Kuramochi, M. Mizuguchi, F. Takano, Y. Semba, H. Akinaga: *Surf. Sci.* **556**, 33 (2004).
- [8] M. Pavúk, M. Miglierini: In: *MEASUREMENT 2011, Proceedings of the 8<sup>th</sup> International Conference on Measurement*, J. Maňka, V. Witkovský, M. Tyšler, I. Frollo (eds.), 27-30 April 2011, Smolenice, Slovak Republic, 188 (2011), ISBN 978-80-969-672-4-7.
- [9] N. Amini, M. Miglierini, J. Dekan, M. Pavúk, P. Novák, S. Habibi: to be submitted for publication, 2017.
- [10] H. N. Ok, A. H. Morrish: *Phys. Rev. B* **23**, 2257 (1981).
- [11] G. Herzer, H. R. Hilzinger: *J. Magn. Magn. Mater.* **62**, 143 (1986).
- [12] U. Köster, B. P. Witteler, G. Steinbrink: *Key Eng. Mater.* **40-41**, 53 (1990).
- [13] M. Miglierini, M. Pavúk: *Acta Phys. Pol. A* **126**, 124 (2014).
- [14] M. Miglierini, T. Hatala, M. Bujdoš: *Acta Phys. Pol. A* **126**, 56 (2014).